Arabian Journal of Chemistry (2022) **15**, 104149

King Saud University

Arabian Journal of Chemistry

www.ksu.edu.sa
www.sciencedirect.com

REVIEW ARTICLE

Acid- and anion-targeted fluorescent molecularly imprinted polymers: Recent advances, challenges and perspectives

Xiaotong Yao

Shandong University Library, Shandong University, Jinan 250100, PR China

Received 30 March 2022; accepted 20 July 2022
Available online 26 July 2022

KEYWORDS

Molecular imprinting;
Acids;
Anions;
Fluorescence;
Sensors

Abstract Acids and anions are important natural components that distribute in plants, animals and products from biotechnological processes. They are usually non-toxic, however, with an increase or decrease in their concentration due to pollution, overuse, chemical reaction etc., acids and anions show harmful effects. Therefore, the detection of acids and anions with high sensitivity and selectivity is necessary. Molecularly imprinting, a technique creating template-tailored cavities in polymer matrices through covalent or non-covalent bonds, has been adapted for the detection of acids, anions and their derivatives. Particularly, fluorescent molecularly imprinted polymers (fMIPs) appear as one of the most promising candidates for chemical sensing due to the high sensitivity and ease of operation of fluorescence. This review summarizes the types of fMIPs, gives an overview of acid and anion templates and features of fMIPs, highlights studies of interest with an emphasis on fluorescent monomers (FMs) used in the synthesis, and finally discusses the challenges and future perspectives.

1. Introduction

Based on Brønsted acid theory, an acid is a molecule or ion capable of disassociating a proton, and consequently forming an anion, such as HX and X^- (X = F, Cl, Br, I), H_2CO_3 and CO_3^{2-}, HCO_3^-, HNO_3 and NO_3^-, H_3PO_4 and PO_4^{3-}, HPO_4^{2-}, $H_2PO_4^-$, H_2SO_4 and SO_4^{2-}, HSO_4^-, $HClO_4$ and ClO_4^-, $HMnO_4$ and MnO_4^-, HCOOH and $HCOO^-$, CH_3COOH and CH_3COO^-, and so on. Acids, anions and their directives (e.g., acid- and anion-containing molecules) are amongst the most pervasive species in nature, that play significant roles in physics, biology and chemistry. The analysis of acids and anions becomes thus important and has been drawn great attention of chemists and biologists (Annak, 2007; Geddes, 2001; Dezfulian, 2007; Mary, 2018).

Only anions show specific physical and chemical properties when acids dissociated (Li, 2010), the sensing of anion moieties thus becomes the key of the development of analytical approaches for acids and anions. In contrast to cations, many of which are normally monoatomic, densely charged, inorganic and brightly coloured, and can be simply detected and quantified by spectroscopical methods such as UV–vis spectroscopy, the direct detection of anions with spectroscopical methods has been proven difficult (Lou, 2012). While the importance of analysis of anions is irrefutable, powerful analytical tools

E-mail address: yaoxt@sdu.edu.cn

Peer review under responsibility of King Saud University.

Production and hosting by Elsevier

https://doi.org/10.1016/j.arabjc.2022.104149
1878-5352

targeting anions in (bio)chemical and biological studies are therefore in highly demanded. Among these analytical tools, molecularly imprinted polymers (MIPs) have emerged as a promising approach for (bio)-chemical detection due to their low-cost, high stability, reusability, high affinity and selectivity (Haupt et al., 2020; Tva, 2020).

Although the developmental history of molecularly imprinting can be dated back 1890′s when Fischer proposed the nature of the enzyme-substrate recognition is analogous to the key-to-lock pattern, the first practical case of molecularly imprinting was on 1931, the Ukrainian scientist Polyakov reported the silica particles synthesized by sodium silicate in presence of organic chemicals, such as benzene, showed preferable bindings to the additive (Polyakov, 1931). In 1942, Pauling and co-workers reported the preparation of artificial antibodies using methyl blue dye as the antigen (e.g., template) (Pauling and Campbell, 1942), inspiring Dickey in 1949 prepared silica-based 'adsorbents' having specific affinities for predetermined substances, e.g., the methyl orange dye and some of its homologs (Dickey, 1949), These methyl orange-imprinted adsorbents were believed to be the first case of MIPs, since the terms of 'pockets', 'foreign molecule' and 'adsorption power' were used to describe such phenomenon, and author indicated these silica materials can be possibly applied for the separation of optical isomers and catalyzing reactions by specific adsorbents of the reactants or products (Dickey, 1955).

MIPs in combination with fluorescent molecular probes are gorgeous, since covalently embedded fluorescent monomers (FMs) allow for direct indication of a rebound template and provide a wealth of information regarding the binding state of fMIPs through the multitude of fluorescence parameters accessible. As the first fMIPs paper was reported in 1998 (Turkewitsch, 1998), not only many fMIPs platforms have been established but also various sensing mechanisms of FMs and templates have been proposed for the preparation of fMIP-based sensors. Considering the effect of the new Coronavirus (COVID-19) outbreak since December 2019, MIP studies have been attracting great interests of chemists, as indicated by the increasing number of MIP literatures and patents (Fig. 1). Moreover, the percentage of fMIP literatures and patents shows that fMIP has been one of the hot topics in MIP research.

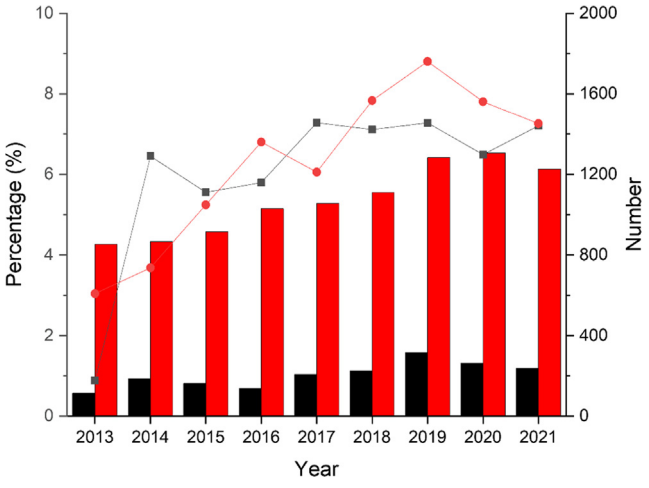

Fig. 1 Numbers of MIP literatures (red bar) and patents (black bar), and the percentage of fMIP literatures (red dot) and patents (black dot) from 2013 to 2021. For literature search: the data was obtained by simple search from Web of Science (WoS) with keywords of '*molecularly imprinted polymers*' and '*fluorescent molecularly imprinted polymers*', respectively. For patent search: the data was obtained by simple search from World Intellectual Property Organization (WIPO) with keywords of '*molecular* imprint**' and '*fluorescen* imprint**', respectively.

To the best of my knowledge, acid- and anion-targeted fMIPs that are used in the detection of important templates, such as biomolecules, drugs of abuse, and explosives, driving toward applications of this technology in medical, (bio)chemical and (bio)analytical research have not been summarized. Therefore, in this review, after the introduction of fMIPs, recent advances of acid- and anion-targeted fMIPs were summarized, including types of template molecules, synthesis strategies, interaction mechanisms, the future trends and challenges were discussed as well.

2. Types of fluorescent MIPs (fMIPs)

Considering the feature of MIPs and fluorescence, it is not hard to come up an idea of doping fluorescent composites into MIP matrix, with the purpose of tracking target molecules (Henry et al., 2005). In addition, integrating polymerizable FMs, which interact with templates covalently or non-covalently, into a MIP shell is another approach for both qualitative and quantitative analysis (Liu, 2019). Consequently, fMIPs can be divided into three types (Fig. 2), e.g., fluorescent composite-doped fMIPs, FM-containing fMIPs, and dual fluorescent MIPs (a fluorescent core coated with a fMIP shell).

2.1. Fluorescent composite-doped fMIPs

Fluorescent composites, including organic composites, such as fluorescent dyes (Guo, 2014), carbon nanodots (CNDs), and inorganic materials, such as quantum dots (QDs), have been greatly developed and used as dopants or functional monomers in the fabrication of fluorescent materials, in particular, fMIPs.

Thanks to the development of organic synthesis, new fluorophores have been synthesized and more fluorescent dyes become commercially available, which allows for embedding high quantum yield fluorescent dyes, such as fluorescein and rhodamine directives (Zhang, 2017), into fMIP matrix becomes one of the most commonly used fMIP patterns. Quantum dots (QDs) are semiconducting nanocrystals whose electronic and optical properties are controlled by their sizes (usually smaller than 10 nm in diameter) and shapes. After the early studies in 1980 s, various QDs, whose fluorescence ranges from blue to red, have been synthesized and applied in biology, such as labelling of cells, quantum dot solar cells, quantum dot displays and emitters of fMIPs (Bimberg et al., 1999). Carbon nanodots (CNDs) are a type of fluorescent carbon-based nanoparticles, with the diameter below 10 nm, which were firstly synthesized in 2004 (Xu, 2004), emitting strong fluorescence (Φ_f can reach up to 90 %), and can be fabricated in green-chemistry ways at large scale (Wang and Qiu, 2016). Possessing above properties, and low toxicity and good biocompatibility, renders CNDs one of the most promising fluorescent nanomaterials for bioimaging, biosensor, drug delivery, and functional monomers and dopants of fMIPs (Zu, 2017).

Upconversion nanoparticles (UCNPs), which are typically made of inorganic host molecules and lanthanide dopants that are embedded within the host's lattice, convert photons from lower energy state to a higher energy state via chemical and physical processes (Wen, 2018). Similar to CNDs, UCNPs exhibit various chemical and biomedical application examples, duo to their high biocompatibility and small dimension, yet

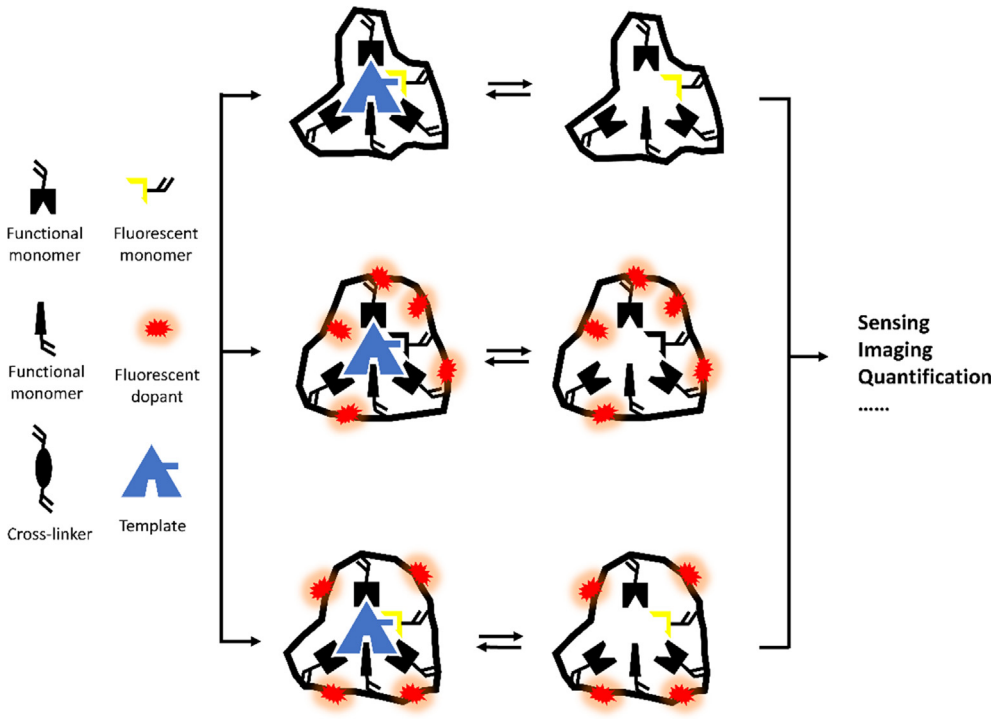

Fig. 2 Three types of fMIPs. (From top to bottom: FM-containing fMIPs, fluorescent composite-doped fMIPs, and dual fluorescent MIPs).

not as many as QD- and CND-doped fMIPs have been published (Jin, 2018).

2.2. Fluorescent monomer (FM)-containing fMIPs

When a polymerizable unit and a recognition group are both introduced to a fluorescent dye, such fluorescent dye can thus be used as a FM for the synthesis of fMIPs, where the recognition of a template by a mixture of monomers and cross-linkers is transduced into a measurable signal (Liu, 2011). A plausible sensing mechanism of FMs and templates should be designed, and further examined by the spectroscopic studies (at micromolar level). Before MIP synthesis, to confirm that whether proposed interaction will occur at millimolar level (e.g., same as MIP synthesis), prepolymerization studies should be conducted (Jiang, 2007). Analytical performance of fMIPs, such as binding affinity and specificity, can be evaluated by fluorescence titrations, e.g., adding the template and competitor compounds to fMIPs at various concentrations (Wang, 2021).

2.3. Dual fluorescent MIPs

Quantification of the target analyte using only the fluorescence emission intensity in a certain wavelength range can sometimes be problematic, because interferences can arise from a variety of analyte-independent factors, such as the light scattering by the sample matrix, excitation source fluctuation, the microenvironment around the probe and variation of the local concentration of the probe.

Thus, the advance of dual fluorescent MIPs is that the fluorescence from the core, which remains unchanged upon the rebinding of template molecules, will serve as an internal reference to calibrate the fluorescence intensity of the fMIP shell for not only quantification of template analyte but also *in vitro* and *in vivo* immunofluorescence staining. The first dual fluorescent MIP case has been synthesized in 2017, aiming at the determination of diniconazole, a triazole fungicide, in soil samples (Amjadi and Jalili, 2017). A widely adopted dual fluorescent MIP preparation method is to coat a fMIP shell onto a fluorescent core. Under single excitation, the resulted fMIPs will emit dual fluorescence, e.g., one from the fluorescent core, the other from the fMIP shell.

3. Templates of acid- and anion-targeted fMIPs

Templates always play a decisive role in a MIP recipe, because, on one hand occurrence and concentration of template molecules in real samples and application scenarios will determine the fMIP architecture, for instance, using a core–shell structured fMIP for rapid sensing and imaging (Yan et al., 2013; Rajpal et al., 2021). On the other hand, in a fMIP recipe, functional monomer(s), co-monomer(s) and cross-linker(s) should be compatible with chemical and physical properties of the template, to avoid poorly defined binding cavities caused by template-monomer reaction and template decomposition (Kupai, 2017; Lin and Yamada, 2000). As summarized in Table 1, acid- and anion-containing molecules, which are of biological, medical and environmental importance, have been considerably imprinted, and resulted fMIPs have been further applied to quantification, adsorption and imaging.

3.1. Biomolecules

Biomolecules consist of glycoproteins, nucleic acids, glycans and their oligomers and monomers, such as amino acids,

Table 1 Summary of acid- and anion-targeted fMIPs.

No.	Anion type	Template	Fluorescence source [a]	Responsive (R) or non-responsive (N)	Interaction mechanism	MIP structure	Application	Ref.
1	Phosphate	Phospholipids	FM ^{S}	R	H-bonds	Core-shell nanoparticle	Sensing	(Li, 2020)
2		Phosphorylated tyrosine	QD ^{D}	R	PET	Core-shell nanoparticle	Quantification	(Amiri and Hosseini, 2020)
3		Amifostine	CND ^{S}	R	PET	Core-shell nanoparticle	Quantification	(Ke et al., 2020)
4		Phosphorylated tyrosine	QD ^{S}	R	PET	Core-shell nanoparticle	Quantification	(Li, 2015)
5		Phosphorylated tyrosine	FM ^{S}	R	ESPT	Core-shell nanoparticle	-	(Wan, 2017)
6		cAMP	FM ^{S}	R	Electrostatic and aryl stacking interactions	Bulk polymer	-	(Turkewitsch, 1998)
1	Sulphate	PFOS	QD ^{S}	R	PET	Hydrogel	Quantification	(Jiao, 2018)
2		PFOS	UCNP ^{S}	R	PET	Mesoporous core–shell nanoparticle	Quantification	(Li, j., 2020)
3		PFOS	FITC ^{S}	R	PET	Core-shell nanoparticle	Quantification	(Feng, 2014)
4		PFOS	UCNP ^{S}	R	PET	Core-shell nanoparticle	Quantification	(Tian, 2021)
5		Tartrazine	CND ^{S}	R	FRET	Hydrogel	Quantification	(Zoughi, 2021)
1	Carboxylate of amino acid	*N*-Cbz-L-phenylalanine	FM ^{S}	R	H-bonds	Bulk polymer	Sensing	(Wagner, 2013)
2		L-Cysteine	FM ^{S}	R	Reaction	Bulk polymer	Quantification	(Cai, 2014)
3		L-Cysteine	QD ^{S}	R	Unspecified	Core-shell nanoparticle	Quantification	(Chao et al., 2014)
4		Oligopeptides	Fluorescein ^{S}	R	Unspecified	Bulk polymer	Sensing	(Piletska, 2020)
5		L-Tryptophan	QD ^{S}	R	FRET	Hydrogel	Quantification	(Tirado-Guizar et al., 2016)
6		*N*-Cbz-L-phenylalanine	FM ^{S}	R	H-bonds	Core-shell nanoparticle	Sensing	(Wan, 2013)
7		L-Histidine	Fluorescent dye ^{S}	R	Coordination bonds	Bulk polymer	Sensing	(Uzun, 2013)
1	Carboxylate of carbohydrate	SA	Pdots ^{S}	N	Covalent bonds	Core-shell nanoparticle	Imaging	(Liu, 2017)
2		GA	Fluorescent dye ^{S}	N	Electrostatic interaction	Core-shell nanoparticle	Imaging	(Rangel, 2019)
3		GA	CND ^{S}	N	Electrostatic interaction	Core-shell nanoparticle	Imaging	(Demir, 2018)
4		GA and SA	QDs and fluorescent dye ^{D}	N	Electrostatic interaction	Core-shell nanoparticle	Imaging	(Panagiotopoulou, 2017)
5		SA	FM ^{S}	R	H-bonds	Core-shell nanoparticle	Imaging	(Shinde, 2015)
6		GA and SA	CND and fluorescent dye ^{D}	N	Electrostatic interaction	Core-shell nanoparticle	Imaging	(Panagiotopoulou, 2016)
7		SA	Fluorescent dye ^{S}	N	Covalent bonds	Core-shell nanoparticle	Imaging	(Wang, 2016)
8		GA	Fluorescent dye ^{S}	N	Electrostatic interaction	Core-shell nanoparticle	Imaging	(Kunath, 2015)
9		SA	FM ^{S}	R	H-bonds	Core-shell nanoparticle	Imaging	(El-Schich, 2016)
10		SA	FM ^{S}	R	H-bonds	Core-shell nanoparticle	Imaging	(Kimani, 2021)
11		GalNAc	Fluorescent dye ^{S}	N	Covalent bonds	Core-shell nanoparticle	Imaging	(Ren, 2021)
12		SA	FM ^{S}	R	H-bonds	Core-shell nanoparticle	Imaging	(El-Schich, 2021)
1	Other carboxylates	2,4-D	FM ^{S}	R	PET	Bulk polymer	Quantification	(Limaee, 2020)
2		Caffeic acid	CND ^{S}	R	PET	Hydrogel	Quantification	(Xu, 2018)
3		*p*-Coumaric acid	QD ^{S}	R	PET	Core-shell nanoparticle	Quantification	(Long, 2019)

Table 1 (*continued*)

No.	Anion type	Template	Fluorescence source [a]	Responsive (R) or non-responsive (N)	Interaction mechanism	MIP structure	Application	Ref.
4		Aristolochic acid I	CND and fluorescent dye ^{D}	R	PET	Core-shell nanoparticle	Imaging	(Ye, 2020)
5		Salicylic acid	Fluorescent dye ^{S}	R	Unspecified	MIP membrane	Quantification	(Meng, 2019)
6		Sinapic acid	CND and QD ^{D}	R	PET	Hydrogel	Quantification	(Zhu, 2021)
7		Folic acid	QD ^{D}	R	PET	Hydrogel	Quantification	(Yang, 2020)
8		2,4-D	QD and FM ^{D}	R	Unspecified	Core-shell nanoparticle	Quantification	(Xu et al., 2020)
9		Okadaic acid	QD ^{S}	R	PET	Hydrogel	Quantification	(Zhang, 2020)
10		Ferulic acid	QD ^{S}	R	PET	Hydrogel	Quantification	(Wang, 2019)
11		Ferulic acid	QD ^{S}	R	PET	Hydrogel	Adsorption and quantification	(Wang et al., 2019)
12		Ciprofloxacin	QD ^{S}	R	PET	Hydrogel	Quantification	(Yuphintharakun, 2018)
13		Folic acid	QD ^{S}	R	PET	Hydrogel	Quantification	(Ensafi et al., 2017)
14		Folic acid	QD ^{S}	R	PET	Bulk polymer	Quantification	(Yang, 2016)
15		Cholic acid	FM ^{S}	R	ICT and PET	Bulk polymer	Quantification	(Xu, 2016)
16		2,4-D	FM ^{S}	R	Electrostatic interaction	Bulk polymer	Sensing	(Ton, 2015)
17		Ascorbic acid	QD ^{D}	R	PET	Bulk polymer	Quantification	(Yang, 2021)
18		Norfloxacin	QD ^{S}	R	PET	Hydrogel	Quantification	(Shi, 2019)
19		2,4-D	FM ^{S}	R	H-bonds	Core-shell nanoparticle	Quantification	(Wagner, 2018)
20		2,4-D	FM and QD ^{D}	R	Unspecified	Bulk polymer	Quantification	(Hou, 2020)
21		Aspirin	QD ^{S}	R	PET	Hydrogel	Quantification	(Wei, 2015)
22		2,4-D	QD ^{S}	R	PET	Core-shell nanoparticle	Quantification	(Jia, 2017)
23		Ciprofloxacin	Fluorescent dye ^{S}	R	Unspecified	Core-shell nanoparticle	Quantification	(Li, 2019)
24		2,4-D	FM ^{S}	R	PET	Hydrogel	Sensing	(Leung et al., 2001)
25		2,4-D	FM and QD ^{D}	R	PET	Core-shell nanoparticle	Quantification	(Wang, 2016)
26		Cephalexin	QD ^{S}	R	PET	Core-shell nanoparticle	Quantification	(Chen, 2020)
27		2,4-D	FM ^{S}	R	PET	MIP membrane	Quantification	(Limaee, 2019)
1	Phenolic compound	2,4,6-TCP	FM ^{S}	R	$\pi - \pi$ stacking	Core-shell nanoparticle and hydrogel	Quantification	(Lu, 2020)
2		2,4,6-TNP	FM and QD ^{D}	R	RET	Core-shell nanoparticle	Quantification	(Li et al., 2017)
3		Paracetamol	Pdots ^{S}	R	Charge transfer	Bulk polymer	Quantification	(Wang, 2020)
4		Salbutamol	QD ^{S}	R	PET	Hydrogel	Quantification	(Raksawong, 2017)
5		4-nitrophenol	CND ^{S}	R	PET	Hydrogel	Quantification	(Wang, 2020)
6		4-nitrophenol	FM ^{S}	R	PET	Hydrogel	Quantification	(Dai, 2020)
7		4-nitrophenol	CND ^{S}	R	PET	Hydrogel	Quantification	(Hao, 2016)

[a] Dual- and single-signal fMIPs are marked with D and S, respectively. Abbreviations: 2,4-D: 2,4-dichlorophenoxyacetic acid, ESPT: excited-state proton transfer, FM: fluorescent monomer, FRET: Förster resonance energy transfer, GA: glucuronic acid, ICT: intramolecular charge transfer, PET: photoinduced electron transfer, PFOS: perfluorooctane sulphonate, RET: resonance energy transfer, SA: sialic acid, 2,4,6-TCP: 2,4,6-trichlorophenol, 2,4,6-TNP: 2,4,6-trinitrophenol.

monosaccharides and nucleotides. Glycoproteins are multifunctional biomolecules that distributed in various biological and physiological aspects, and thus glycoprotein-targeted fMIPs have been synthesized and avidly utilized in health-related studies (Takeuchi et al., 2007). Considering the fact that not only the interaction between carboxylic acid (and/or carboxylate) of glycoproteins with monomers, but also many other factors (such as pH, salt concentration and the charge state of protein) are contributing to imprinting of glycoproteins (Whitcombe, 2011; Chen, 2019), in this review, glycoprotein-targeted fMIPs are not discussed.

Comparing with intact proteins, amino acids are relatively small and compatible with organic porogens, and thus can be used directly in imprinting process as simple organic compounds. For instance, L-cysteine, an amino acid plays significant roles in cellular detoxification and metabolism (Alcock et al., 2018), was imprinted with the aim at isolation and quantification of cysteine-containing peptides from real samples (Cai, 2014; Chao et al., 2014). Wan, et al. synthesized a urea-containing nitrobenzoxadiazole (NBD)-based FM for the imprinting of benzyloxy carbamate (Cbz) protected L-phenylalanine (*N*-Cbz-L-phenylalanine, Z-L-Phe). Upon addition of Z-L-Phe to the prepared core–shell fMIPs, fluorescence increase was observed, whereas fluorescence quenching suffered from unspecific competitors rebound, yielding an imprinting factor (IF) of 3.6 (Wan, 2013). Another Z-L-Phe-fMIPs were prepared by Wagner, et al (Wagner, 2013) Analogous to the NBD-based FM, a naphthalimide-based FM was synthesized and further integrated into bulk Z-L-Phe-fMIPs. An IF of 3.4 was obtained via spectroscopical studies. Moreover, after immobilization of Z-L-Phe-fMIPs on glass coverslips, thin-film fMIP-based sensors showed a clear enantioselective fluorescence quenching dependence and a discrimination against competitive protected amino acids.

Protein phosphorylation is one of the most common post-translational modifications (PTMs) on tyrosine, serine and threonine moieties, regulating protein interactions and coordinating various cellular pathways (Watanabe and Osada, 2016). Phosphorylated amino acids have been regarded as important biomarkers and consequently served as templates of fMIPs. Besides CND- and QD-containing fMIPs (Amiri and Hosseini, 2020; Li, 2015), it is noted that a silica core-fMIP shell ratiometric nanosensor, that decorated with a responsive bis-urea-containing FM, allowed for the selective detection of phosphorylated tyrosine (Wan, 2017). Upon addition of the template, fluorescence increase and a second red-shifted emission band were observed, yielding an IF of 3.7. More importantly, in combination of fMIP-based detection with a phase-transfer assay, the IF was further improved to 15.9, enabling the determination of phosphorylated tyrosine in aqueous media.

Nucleic acid-targeted MIPs have been greatly synthesized, whereas no fMIP platform, in which used the interaction between the phosphate moiety and FMs, was developed. Until 1998, a cAMP-imprinted fluorescent polymers was reported, where Turkewitsch, et al. described the synthesis of cAMP-fMIPs, in which the phosphate moiety of cAMP rebound to FMs via electrostatic interactions (Turkewitsch, 1998). The electrostatic interactions arising due to positive and negative charges on the FM and cAMP, respectively, played a critical role in the FM-cAMP interaction, allowing for the formation of binding cavities (Fig. 3A). Later on, as illustrated in Fig. 3B, an indirect ATP-sensing method was published (Yang, 2013). Once ATP-fMIP cavities interacted with ATP's adenosine moiety, another fluorescent probe was added to bind to ATP's phosphate moiety. Quantification of ATP was achieved by measuring the fluorescence of added fluorescent probe.

Besides the interaction between phosphate moiety and FMs, it is also possible to sense DNA or RNA by nucleobase pairing. For instance, to quantify 5-fluorouracil (5-FU), an anticancer drug, in real samples, a FM that interacted with 5-FU via the mechanism of RNA-type nucleobase pairing was synthesized, followed by the incorporation into a fMIP layer (Huynh, 2013). Although the LOD of prepared 5-FU-fMIP sensors was relatively high (0.26 mmol L^{-1}), it is sufficient for determination of 5-FU in real samples. More importantly, such interaction mechanism can be potentially used in the fabrication of fMIPs that target other nucleic acids.

Glycosylation is another important PTMs, especially, the altered glycosylation, which is revealed to be associated with disease phenotypes, such as inflammation, Alzheimer disease and cancer. Therefore, several glycan antigens have been regarded as promising targets for biomarkers and therapeutics (Silsirivanit, 2019). Glucuronic acid (GA), *N*-acetylgalactosamine (GalNAc) and *N*-acetylneuraminic acid (sialic acid, SA) have been imprinted, with the aim of cancer cell staining and imaging, since it is believed that GA, GalNAc and SA overexpress on cancer cell membrane due to altered glycosylation. GalNAc and SA contain diol groups, which can be covalently reacted with a boronic acid-containing co-monomer to form a five- or six-membered ring (Liang and Liu, 2011), phenylboronic acid was therefore modified on the surface of nanoparticles, allowing for the boronate-affinity surface imprinting of GalNAc and SA (Wang, 2016; Liu, 2017; Ren, 2021). Fluorescein and fluorescent polymer dots were used as emitters of fMIPs, enabling cancer cells staining and *in vivo* imaging.

Considering the fact that carboxylic acid moiety of sugar acids can form electrostatic interactions with basic functionalities, Haupt and co-workers synthesized a non-fluorescent monomer, 4-acrylamidophenyl)(amino)methaniminium acetate (AB) (Fig. 4) (Kunath, 2015; Panagiotopoulou, 2017; Demir, 2018), and further incorporated AB into a GA-fMIP shell via solid-phase synthesis approach (Rangel, 2019). CNDs, QDs and rhodamine B were used as the emitter for imaging cancer cells *in vitro*. Notably, a simultaneous duplexed labelling of human keratinocytes was achieved with green fluorescent GA-MIP and red fluorescent SA-MIP, suggesting a generic method for the preparation of duplexed fMIPs to be possibly used in more complicated biorecognition scenarios (Panagiotopoulou, 2016).

Besides the direct interaction of carboxylic acid-FM in above cases, the carboxylate state of SA, which was prepared by addition of tetrabutylammonium hydroxide (TBA-OH), was used to form a stable hydrogen-bonded complex with the urea moiety of FMs (Shinde, 2015; El-Schich, 2016; Kimani, 2021; El-Schich, 2021), in a similar way as above Z-L-Phe-fMIP cases reported by Wan, et al. and Wagner, et al. This carboxylate-urea interaction approach was further applied to prepare phospholipid-fMIPs (Li, 2020). To validate the specificity of binding cavities, two pentavalent SA conjugates were synthesized (Johansson, 2020), and significantly reduced the binding of SA to SA-fMIPs in a concentration-

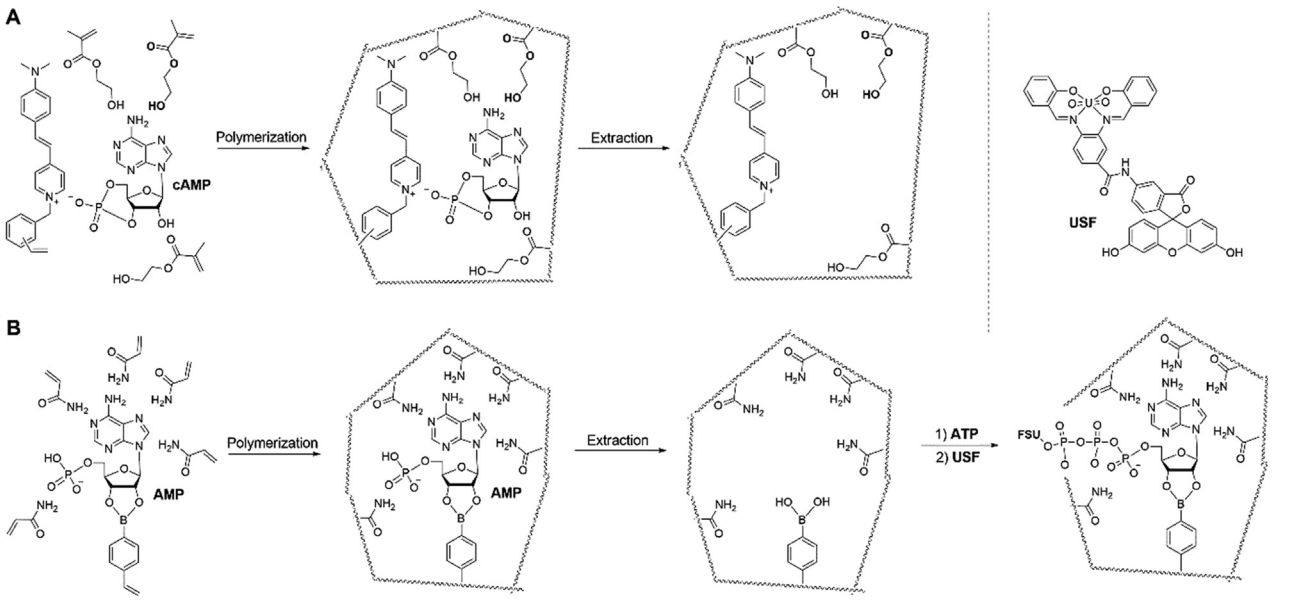

Fig. 3 Schematic representation of hypothetical imprint formation of (A) cAMP-fMIPs and (B) ATP-MIPs. Adapted with permission from reference (Turkewitsch, 1998; Yang, 2013).

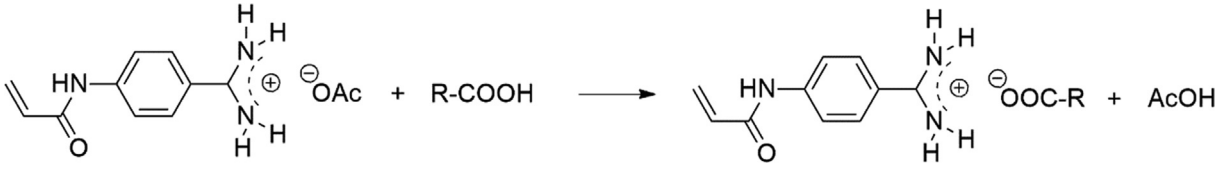

Fig. 4 Electrostatic interaction between 4-acrylamidophenyl)(amino)methaniminium acetate (AB) and carboxylic acids. Adapted with permission from reference (Panagiotopoulou, 2017).

dependent manner (El-Schich, 2021). This indicated SA-fMIPs binding to cancer cells was mediated by the interaction with SA-terminated glycans.

3.2. Antibiotics

Emergence of resistance among the most important bacterial pathogens is recognized as a major public health threat affecting humans worldwide. Moreover, the mechanisms of antibiotic resistance are encoded by genomic changes through various sources (Li et al., 2015), and thus the detection of antibiotics becomes more and more critical. Several fMIPs targeting antibiotics, such as ciprofloxacin, norfloxacin, cephalexin, have been prepared and applied for the quantification of real samples. In the synthesis of fMIPs, carboxylic acid groups of ciprofloxacin (Yuphintharakun, 2018; Li, 2019), norfloxacin (Shi, 2019) and cephalexin (Chen, 2020) were used to interact with QDs via photoinduced electron transfer (PET), which result in fluorescence increase, decrease and shift of emission band. The PET process can be explained that the acid of antibiotics processes an empty orbit, which can accept LUMO electrons of QDs. Therefore, electron can transfer from LUMO to that orbit and then back to ground state, leading to fluorescence quenching. The process is called oxidative electron transfer. Besides QD-doped antibiotic-targeted fMIPs, an Europium(III)-based monomer was synthesized and utilized as the emitter to sense ciprofloxacin (Li, 2019). The limit of detection (LOD) was 0.28 nmol/L and IF was 1.5, suggesting a rapid, selective and sensitive ciprofloxacin-fMIP platform was established, however the fluorescence sensing mechanism of Europium(III) complex and ciprofloxacin remained unspecified.

Quinolone antibiotics contain same pharmacophores, i.e., one carboxylic acid and one quinoline ring, therefore, it is possible that establishing a universal fMIP platform for quinolone antibiotics. QD-doped silica hydrogel can be used as a universal fMIP platform for quinolone antibiotics. Because, on one hand, both ciprofloxacin- (Yuphintharakun, 2018) and norfloxacin-fMIPs (Shi, 2019) selected this fMIP format. On the other hand, cephalexin, being a first-generation cephalosporin, adopted this format as well, with the modification of adding cetyltrimethylammonium bromide (CTAB) in the formation of hydrogel (Chen, 2020). Although the resulted mesoporous silica nanoprobes did not show a better LOD value (2.3 nmol/L) comparing with ciprofloxacin-fMIPs (0.2 nmol/L) (Yuphintharakun, 2018), an improved binding capacity was obtained.

3.3. Hazardous chemicals

Perfluorinated organic compounds (PFOCs), such as perfluorooctane sulphonate (PFOS) and perfluorooctanoic acid

(PFOA), which have been widely used in many industrial and commercial applications, are one type of persistent environmental contaminants and becoming a worldwide pollution problem, due to their high stabilities, bioaccumulation effects and toxicities for plants, animals and human beings (Lau, 2012). As listed in Table 1, PFOS-targeted fMIPs have been already synthesized and exhibited selectivity and sensitivity in the quantification of serum (Jiao, 2018; Li, 2020; Tian, 2021), water (Li, 2020; Tian, 2021; Feng, 2014) and egg extract (Tian, 2021) samples. The interaction mechanism of sulphonate group of PFOS and CNDs was determined as hydrogen bonding or electrostatic reactions, which can enhance the conjugation degree of CQDs. In addition to QD-doped silica hydrogel fMIP platform, a CND-doped chitosan hydrogel PFOS-fMIP system was established. However, the chitosan hydrogel is irreversible, as harsh elution condition (0.5 mol/L NaOH/acetone = 1/1, 8 h) would decrease the cross-linking degree of chitosan, and thus affect binding cavities (Jiao, 2018).

Herbicides are used to control unwanted plants, with little or no impact on other organism in the environment. However, herbicides residues, for instance 2,4-dichlorophenoxyacetic acid (2,4-D) and 2,4,6-trichlorophenol (2,4,6-TCP), in the environment caused by accident or an inappropriate application process, have been found in water, air and soil, leaving healthy and environmental side effects. To meet the demands of rapid, sensitive and selective sensing of 2,4-D, several 2,4-D-fMIPs have been fabricated (Limaee, 2020; Wagner, 2018), among which QDs were selected mostly as the FM to interact with 2,4-D via PET process (Xu et al., 2020; Ton, 2015; Hou, 2020; Jia, 2017; Leung et al., 2001; Wang, 2016; Limaee, 2019). Besides QD-doped fMIPs, Limaee, et al. reported the synthesis of 2,4-D-fMIPs, which incorporated a naphthalimide-based FM that can interact with 2,4-D via H-bonds. Upon addition of the template, a fluorescence decrease was observed. A linear range of $5 \times 10^{-7} - 1 \times 10^{-3}$ mol L^{-1} and a LOD of 16.8 nmol/L of 2,4-D-fMIPs were achieved (Limaee, 2020). Wagner, et al. reported the integration of a silica core-fMIP shell nanoprobe with a droplet-based 3D microfluidics, that enabled a direct analysis of worldwide water samples without sample preparation. Although a relatively high LOD of 4 μmol/L was obtained, an IF of 6.9 and discrimination factors (DFs) against 4-(2,4-dichlorophenoxy)butanoic acid (2,4-DB) and 2-(2,4-dichlorophenoxy)propionic acid (2,4-DP) of 2.0 and 3.0, respectively, showed a good selectivity for 2,4-D analogues (Wagner, 2018).

Regarding 2,4,6-TCP-fMIPs, Lu, et al. synthesized an ionic liquid-type FM and further incorporated into a MIP shell with co-monomers and cross-linkers on the surface of silica nanoparticle cores. The resulted fMIPs showed a linear range of 0.1–50 nmol/L, a LOD of 89 pmol/L and a detection time of ca. 1.5 min, indicating a rapid, sensitive and selective quantification of 2,4,6-TCP in industrial wastewater was accomplished with fMIP-based nanoprobes (Lu, 2020). Above 2,4-D- and 2,4,6-TCP-fMIP cases suggest that few-nanometer thin MIP layers guarantee fast equilibration time, which is essential for instance for hazardous chemical detection assays (Fig. 5). Moreover, the core–shell structure would allow for the fabrication of dual fluorescent MIPs by doping the silica core with fluorophores.

3.4. Toxins

Toxins in food are becoming one of the serious threats to human health. Once these toxins enter human bodies, they would compromise the immune system and consequently cause many physical problems (Delaunay et al., 2020). Okadaic acid (OA), a natural polyketide, and its derivatives are known as inhibitors of the serine/theorine protein phosphatases PP1 and PP2A, and thus have been regarded as a tumor promoter (Forsyth, 2002). Zhang, et al. reported the analysis of OA with fMIP-based sensors. QDs were used as the emitter, which were coated with a silica MIP shell, allowing for the specific recognition of OA in aqueous media. Upon addition of OA, a fluorescence quenching was observed, resulted from a PET process between OA and QDs. A linear relationship of 10.0–100.0 mg kg^{-1} and a LOD of 0.25 mg kg^{-1} were achieved in the quantification of OA in the shellfish samples (Zhang, 2020). Aris-

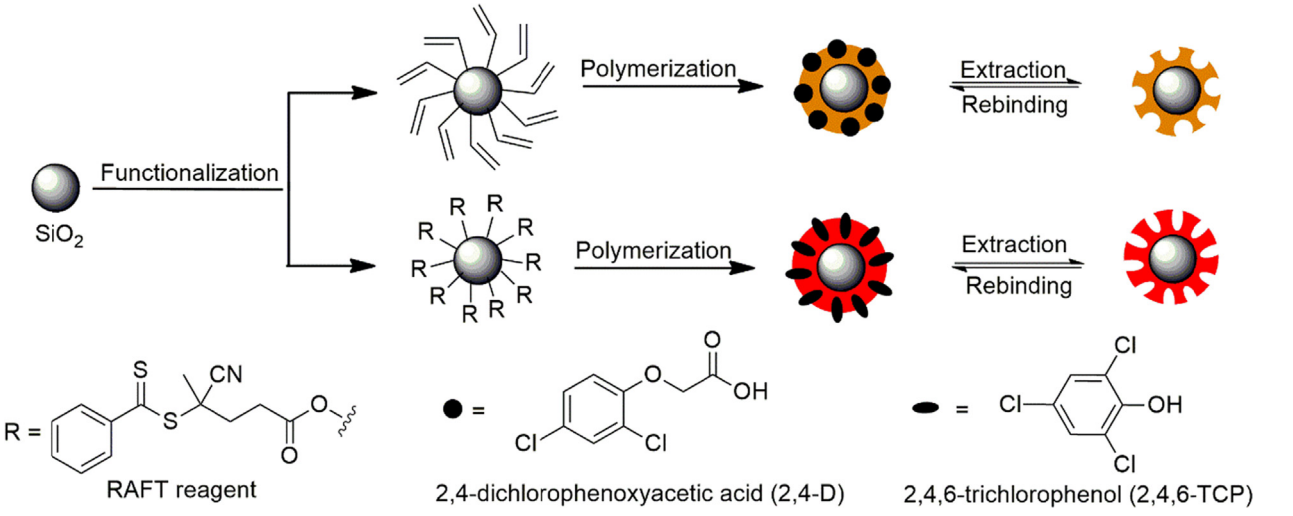

Fig. 5 Schematic illustration of preparation procedures of silica core-fMIP shell structured 2,4-D- (Wagner, 2018) and 2,4,6-TCP-fMIPs (Lu, 2020).

tolochic acids (AA) are a type of natural products isolated from the family Aristolochiaceae and commonly used in traditional Chinese medicine (TCM), among which aristolochic acid I (AAI) is the most abundant and toxic one (Han, 2019). Ye, et al. reported the fabrication and application of AAI-imprinted ratiometric fMIPs. A Schiff-base type FM was doped into silica nanoparticles, on which a CND-containing fMIP layer was immobilized. The interaction mechanism of CND and AAI was determined as PET. Under the optimum condition, the emission band at 530 nm was quenched in the range 1.0–120.0 μmol L^{-1}, whereas the referenced fluorescence of Schiff-base type FM at 440 nm remained unchanged. The LOD was determined as 0.45 μmol L^{-1}, and an IF of 2.25 (Ye, 2020).

Although a large number of OA and AA analogues have been isolated from natural sources, the *in vitro* toxicity has only been reported for part of these compounds (Michl, 2014). Therefore, typical analogues of OA and AA (Fig. 6) can be targeted and further studied with fMIPs. Additionally, inorganic toxic acids and carboxylates that are isolated from TCMs can be imprinted as well, with the aim of the preparation of sensors and adsorbents (Xu, 2020).

3.5. Phenolic compounds

Phenols and phenolic compounds, which usually show antioxidant activity, are commonly acidic, due to the deprotonation of hydroxyl forms a proton and a phenolate anion correspondingly. Besides the hydroxyl group, phenolic compounds lack unique structural characteristics for binding specificity, therefore, the preparation of selective phenolic compound-targeted fMIPs remains challenging. Analogous to acid- and anion-fMIPs, QDs and CNDs were selected as FMs to interact with phenolic compounds via PET in the targeting of most phenolic compounds, including caffeic acid (Xu, 2018), sinapic acid (Zhu, 2021), ferulic acid (Wang, 2019; Wang et al., 2019), salbutamol (Raksawong, 2017), 4-nitrophenol (Wang, 2020; Dai, 2020; Hao, 2016) and 2,4,6-trinitrophenol (2,4,6-TNP) (Li et al., 2017). In addition, $\pi - \pi$ stacking and charge transfer were interaction mechanisms of 2,4,6-TCP- (Lu, 2020) and paracetamol-fMIPs (Wang, 2020), respectively.

4. Fluorescent monomers of acid- and anion-targeted fMIPs

Besides the template, FMs play decisive roles in the synthesis of fMIPs, since they can directly indicate the rebinding of template molecules, and thus provide a various of information regarding not only the binding state but also the analytical performance of fMIPs. CNDs and QDs have been mostly applied as FMs to interact with the template via PET process (Table 1), whereas, when an interaction functionality is introduced a fluorescent dye, the resulted derivative would serve as a FM to be incorporated into the fMIP layer. As shown in Fig. 7, five types of interaction functionalities, e.g., urea, secondary and tertiary amine, quaternary ammonium cation and Schiff base, modified on fluorophores, yielding 15 compounds that showed fluorescent response to acids or anions via covalent/non-covalent interactions.

Urea, which has both H-bond acceptor (e.g., carbonyl group) and donor (e.g., two hydrogen atoms) is an ideal functionality for acids and anion sensing, since the former has the tendency to accept protons from acids, while the latter would donate protons to interact with carboxylate, carbonyl group and other anions (Duke, 2010). Consequently, the formation of H-bonds is largely related to the acidity of urea and acid/-carboxylate. Therefore, the urea moiety of nitrobenzoxadiazole (NBD) (Wan, 2013), naphthalimide (Wagner, 2013), phenoxazinone (Wagner, 2018) and phenazine derivatives

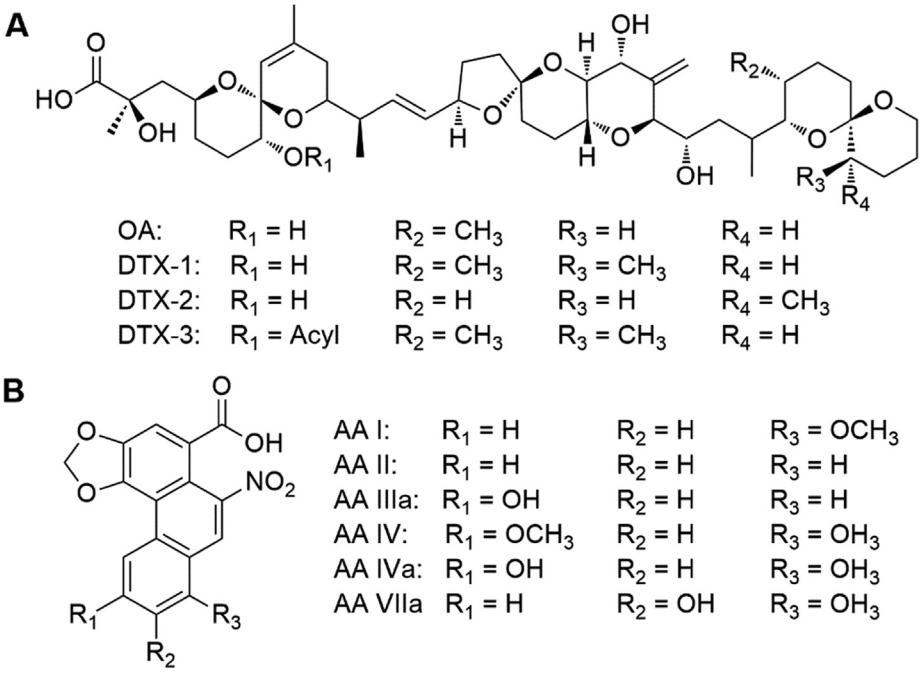

Fig. 6 Chemical structures of (A) okadaic acid (OA) and dinophysistoxins (DTXs) and (B) aristolochic acid (AA) and some typical analogues.

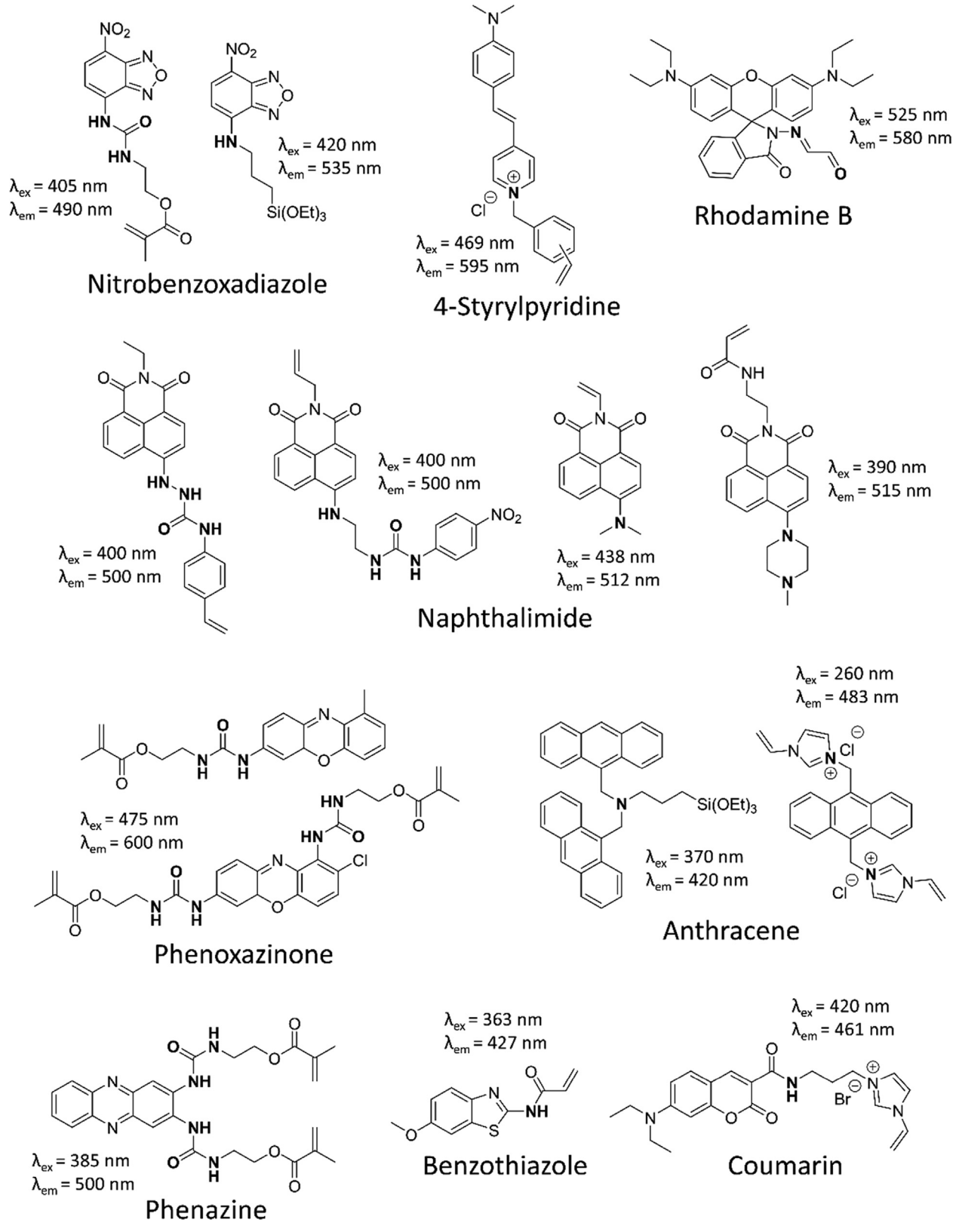

Fig. 7 FMs in the synthesis of fMIPs targeting acids and anions.

(Wan, 2017), which emit at 490–600 nm, have been proved to interact with carboxylic acids or carboxylates via H-bonds. The logK_{on} values were determined at the range of 3.7–5.1, indicating a strong interaction affinity of FMs to carboxylate and phosphate. These urea-containing FMs can be synthesized within three steps, in which the condensation reaction between

a primary amine and an isocyanate not only forms the urea moiety, but introduces a polymerizable unit into these molecules.

Secondary amine can work solely as the interaction functionality to probe acids (Wang, 2016; Li et al., 2017), in the way of H-bond donor as urea, however, with a weaker binding affinity than urea. Thus, Limaee, et al introduced both a secondary amine and a urea into a FM for the fMIP-based quantification of 2,4-D (Limaee, 2020). As illustrated in Fig. 8A, 2,4-D rebound to fMIPs via a dual recognition pattern, e.g., secondary amine-phenoxy and urea- carboxylic acid. In the case of 4-nitrophenol targeted fMIPs (Fig. 8B), a coumarin-based FM, of which quaternary ammonium cation assisted the secondary amine to stabilize the proton of 4-nitrophenol, was synthesized for preparing fMIP-sensors. The results of spectroscopical studies indicated a high sensitivity, good selectivity and rapid sensing of 4-nitrophenol with obtained fMIP-sensors (Dai, 2020).

Tertiary amine groups, such as dimethyl- and diethylamino, and 1,4-dimethylpiperazine, and quaternary ammonium cations, such as alkyl-substituted imidazolium and pyridinium, have been widely used to interact with acid moieties, since they show basic property in aqueous environment. Therefore, introducing the tertiary amine group (Ton, 2015; Leung et al., 2001; Xu, 2016) and quaternary ammonium cation (Turkewitsch, 1998; Lu, 2020) by substitution reactions would not only allow acids or anions specifically bind to the FM, but also increase the FM's aqueous solubility. When acid or anion templates approaching the FM in fMIP layers, both deprotonation/protonation of templates and corresponding response of FM's fluorescence would occur, due to the PET process between template's electrons/protons and the nitrogen atom of tertiary amine or quaternary ammonium cation of FM molecules (Fig. 9A).

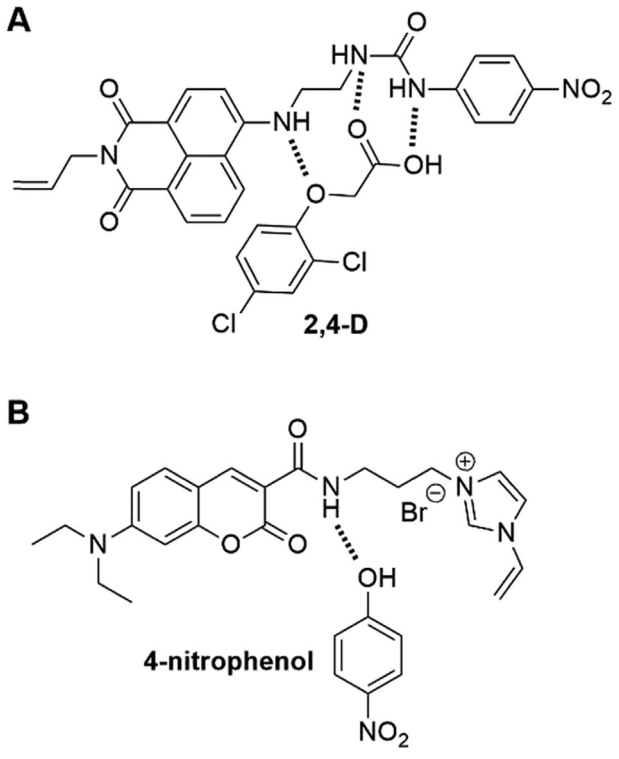

Fig. 8 The illustration of (A) the dual recognition pattern of napthalimide-type FM to 2,4-D and (B) the possible H-bond between coumarin-based FM and 4-nitrophenol. Adapted with permission from reference (Limaee, 2020; Dai, 2020).

Since most acids and anions sensing are performed in aqueous media, which might hamper conducting organic reactions, reaction type FMs, e.g., fluorescence sensing via forming covalent bonds, are not as frequently reported as above non-covalent type FMs. Cai, et al. reported the preparation of fMIP-based sensors which incorporated with a Schiff base type FM for quantification of L-cysteine (Cai, 2014). Upon addition of L-cysteine, an unstable intermediate was formed between aldehyde and L-cysteine, followed by a ring-opening reaction. Lastly, the hydrolysis of ring-opened compound at Schiff base position occurred, accompanied with strong fluorescence and colour change, since a conjugate system was formed (Fig. 9B).

5. Synthesis methods of acid- and anion-targeted fMIPs

The sol–gel based non-covalent method has been adopted mostly in the synthesis of fMIPs, for instance, fluorescent molecularly imprinted silica (fMIS) (Table 1). Nano- or micro-sized fMIS synthesized via the Stöber process is a typical pattern of sol–gel fMIPs (Tirado-Guizar et al., 2016). Basically, tetraethyl orthosilicate (TEOS) and (3-aminopropyl) triethoxysilane (APTES) are regularly used as the cross-linker and functional monomer, respectively. Moreover, a 're-growth' method has been developed, allowing to grow an imprinted silica layer on surface of silanol functionalized QD-doped cores (Xu, 2013). In fMISs, QDs work either as dopants that allow fMIPs to be tracked by fluorescence microscopes, or as FMs to interact with the template. For CND-fMIPs, blue-emissive CNDs have been selected mostly, working similarly as QDs, e.g., dopants for fMIPs. Using QDs or CNDs as FMs to interact with the template becomes a trend in fMIP synthesis, however, due to complexity of functionalities on the surface of CNDs or QDs, the interaction mechanism is still needed further investigation (Singh, 2020).

Another frequently used polymerization method is radical polymerization. For a typical radical polymerization process, everything begins with the birth of free radicals, that are generated from initiators. According to the method of radical generation, radical polymerization can be roughly divided into photo- and thermally initiating types. Benzophenones and benzylketals are often used as photo-initiators, that can be cleaved through irradiation with UV or visible light to form the free radicals. However, it would be not suitable for fMIPs, since it will potentially bleach the FMs through the rather high-energy UV-light. Therefore, the use of photo-initiators can not only avoid FM bleaching, but enable low temperature polymerization, often at 0 ℃. Both azobisisobutyronitrile (AIBN) and 2,2′-azobis(2,4 dimethyl)valeronitrile (ABDV) have been used as thermo-initiators, whose dissociation temperatures are 60 ℃ and 40 ℃, respectively. These two initiators are mostly used in the synthesis of fMIPs.

Comparing with templates and FMs, co-monomers and cross-linkers plays less critical roles in radical polymerization. Methacrylamide (MAa), 2-hydroxyethyl methacrylate, benzyl methacrylate (BMA), methacrylic acid (MAA), acrylic acid, 4-vinylbenzoic acid (VBA), 4-vinylpyridine, *N*-phenyl acry-

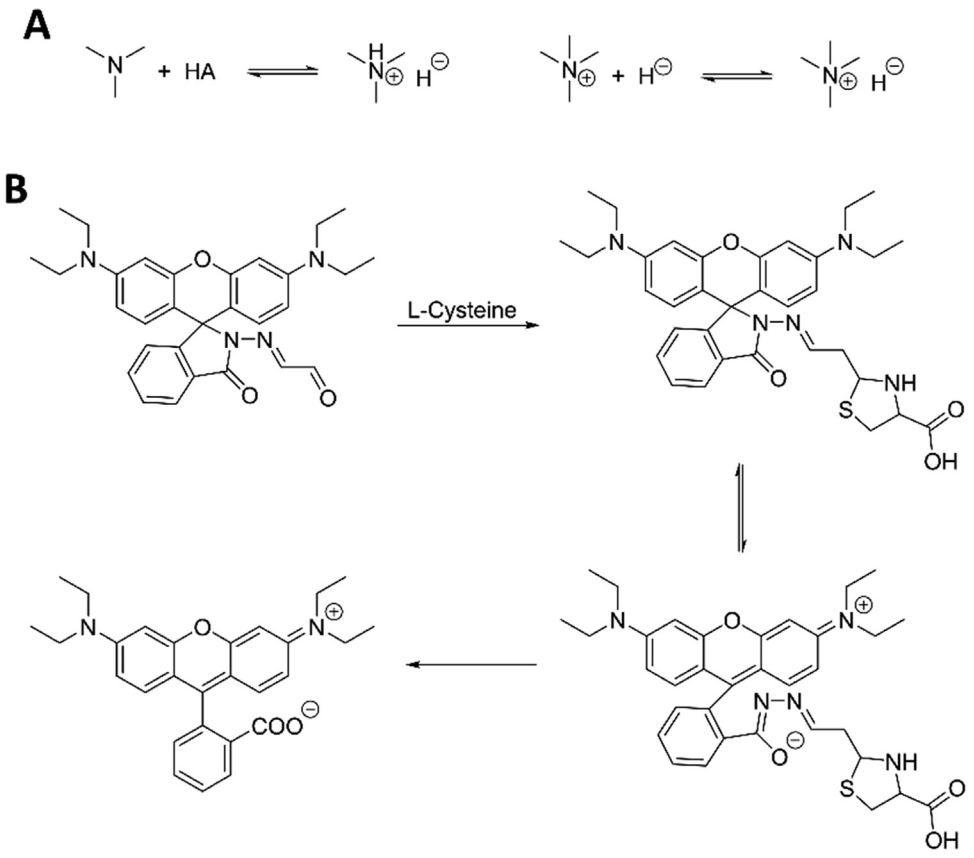

Fig. 9 (A) Equilibria of PET process in the interaction between templates and FMs. (B) Interaction mechanism of fluorescent detection for L-cysteine with reaction-type FM. Adapted with permission from reference (Cai, 2014).

lamide have been used as co-monomers in fMIP synthesis. MAa and 4-vinylpyridine are frequently selected for acid and anion templates, since they show basic property in aqueous media (Friedman, 2001). Ethylene glycol dimethacrylate (EGDMA), trimethylolpropane trimethacrylate (TRIM), *N*, *N*'-methylenebisacrylamide have been used as cross-linkers in fMIP synthesis.

6. Challenges and perspectives

As discussed above, a considerable number of achievements of fMIPs has been obtained, especially in FMs and the synthesis, and yet there are some rooms can be improved in future studies.

One of the challenges in fabrication of fMIPs is the rapid synthesis of FMs, since the most commonly used approach is indirect synthesis, e.g., forming interaction moieties after the amination step, for instance, the synthesis of NBD type FMs (Wan, 2013). This might be limited by the number of commercially available building blocks of fluorophores and polymerizable units. In future research, both the structural diversity of templates and the systematic study of structure-affinity relationship between FMs and templates probably require a direct functionalization approach, e.g., introduce an interaction moiety in one step with high yield (Fig. 10). For instance, when aiming at functionalization of a fluorophore with a guanidine group, which has more electron withdrawing ability than urea and thiourea, a three-step reaction, that contains amination, condensation to urea and reduction to guanidine, would be usually used. It might be feasible to introduce guanidine moiety to NBD halides via a direct guanidinylation, inspired by the research, where Hammoud, et al. reported a modified Ullmann reaction using *p*-methoxybenzyl (PMB) guanidine as guanidinylation agent for the synthesis of heteroaryl guanidi-

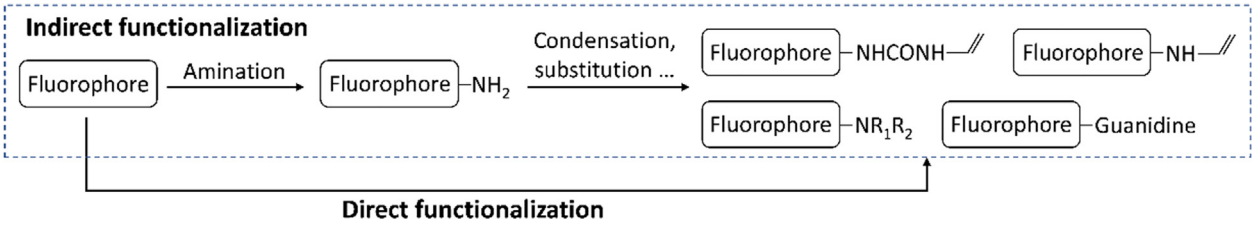

Fig. 10 Current indirect functionalization strategy in the synthesis of FMs (in dash box) and the proposed direct functionalization strategy.

nes (Hammoud, 2012). The methodology of direct functionalization of urea, thiourea, guanidine and other groups should be investigated in future studies.

The orientation of FMs in the MIP matrix is another way to improve fMIP's binding performance, which has not been systematically studied. It would be an interesting research topic for the future, for instance, by modifying the point of integration or introduction of a second polymerizable group, to assess the potential of fluorescent probes. These might not only introduce more fluorogenic monomer into the MIP matrix but also promote the sensing response of the already succeed monomers.

Second, the achievement of higher binding affinity to biomarcromolecules, such as proteins, glycans or even cells, largely relies on using more elaborate target structures, that have various functionalities to interact with FMs, co-monomers and cross-linkers. Moreover, a relatively simple compound used as the template can arise more unspecific bindings, caused by the wide expression of the template molecules. For instance, it is well investigated that normal cell lines express GA and SA, therefore, more cancer specific biomarkers, such as the Thomsen-nouveau (GalNAcα1-*O*-Ser/Thr, Tn) and the sialyl-Thomsen-nouveau (Neu5Acα2-6GalNAcα-*O*-Ser/Thr, Sialy-Tn or STn) antigen, should be used as ideal template molecules for distinguishing cancerous cells from normal ones. However, oligo- and polymers of saccharides and peptides, particularly oligomer of sugar acids and phosphate peptides, are hard to obtain in comparison with their monomers, that would hinder the analytical performance of fMIPs.

For most acid templates, which have excellent water solubility, the deprotonation (e.g., disassociation into anion and proton) should be taken into consideration, especially using the acid form in spectroscopic studies of the interaction between templates and FMs. In the cases of GA and SA, the carboxylic acid moiety is most likely deprotonated ($pK_a = 3.0$ for GA and $pK_a = 2.6$ for SA) and electrostatically associated with inorganic cations (e.g., Na^+, K^+, Ca^{2+}) in physiological buffer when aiming at *in vitro* and *in vivo* studies. Therefore, imprinting of the sodium salt of GA and SA, instead of the acid state, would enable fMIPs to perform better in real scenarios.

Third, additional functional shells on the surface of fMIPs can be introduced, on one hand, to enable additional gating functions. These can be photo-switchable layers or lower/upper critical solution temperature (LCST/UCST) layers to enable photo- or thermal switching of the protecting layer to control access of the analyte to the MIP shell. In natural systems, such as an enzyme, the hydrophobic binding site is protected by the protein backbone. Nature uses a complicated coding system to synthesize a long peptide chain and then fold it into the right ternary structure. However, this is impossible to realize within the structure of a polymer. Although more commercially available monomers can be investigated than nature, a systematic polymerization is difficult. Therefore, mimic the effective position with a limited monomer system and introduce a protective shell in a later step through post-grafting might simplify this problem.

On the other hand, to minimize unspecific bindings, additional shells can be introduced by poly(ethylene glycol) (PEG) modification, particularly for real samples in bioanalysis, where non-target interactions can naturally occur *in vitro* and *in vivo*, due to the high complexity of the application environment (such as serum, plasma and other body fluids) and the characteristics of analyte sample of interest. For instance, in addition to binding to glycans, fMIPs may also recognize other sites on the surface of cells or even adhere to other beads in a purely unspecific way. The strategy of functionalization a PEG shell on fMIPs surface is based on the protein-repelling effect of PEG, due to the low free energy at PEG–water interface, incapability of hydrogen bonding or electrochemical interaction of PEG with glycoproteins, and to the high mobility of PEG chains, and therefore enabling to reduce unspecific bindings (Kingshott and Griesser, 1999).

Fourth, portable fMIP systems, such as microfluidic chips, are very promising sensing patterns for the future. This miniaturized flow system can be easily coupled to portable detection units. With the help of advanced and miniaturized camera system (e.g., webcams, smartphones), true handheld optical sensors can be assembled. Raw data registered by such systems can be directly transmitted through wireless connections and for instance, they can automatically be delivered to a medical centre for further diagnosis and advice. Especially coupled to the nowadays highly developed cloud storage and high-speed internet systems, a remote diagnostic and medical treatment system can be built in the near future. This would be very exciting not only for the patient but also for those people doing daily health monitoring.

Last but not least, with the increasing need of big-data-driven studies, the application format can be elaborated, for instance, a sensor array that can provide more information about the sample under investigation. Regarding high sample throughput, fast and reliable measuring array sensors can greatly improve performance. Array systems can be realized on a slide by depositing different sensor particles in spots onto glass slides and assessing them through an array scanner. Another array format can be realized in liquid phase and processed through flow cytometer. For instance, different barcoded sensor particles can be suspended in solution and mixed with analytes. These particles will pass the detection area and the sensing response will be registered. Additionally, an array system cannot only provide multi-target detection but also increase the dynamic range and simplify the sensing process.

7. Conclusions

In this review article, I attempted to cover all the reported fMIPs and fMIP-based sensors for the detection of acids and anions. It was concluded many types of acid and anion templates have been imprinted with various FMs, resulting in responsive fMPs that rebind to template molecules via various interaction mechanisms. High affinity and specificity, short response time, low LOD, and other promising features have been obtained by using fMIP-based sensors for acid and anion detection in real samples. Based on the modularity of these acid- and anion-targeted fMIPs, the concept can be transferred in a straightforward manner to other target analytes. Further endeavours should be focused on the direct functionalization of FM and development of portable and highthroughput fMIP platform, that will bring fMIP-based sensory materials a brilliant future.

Declaration of Competing Interest

The authors declare that they have no known competing financial interests or personal relationships that could have appeared to influence the work reported in this paper.

Acknowledgement

I thank the Key Technologies R&D Program of Shandong (grant no. 2017GG20002021), National Student Research Training Program (grant no. 11110412089), and Shandong University Library for funding this work.

References

Alcock, L.J., Perkins, M.V., Chalker, J.M., 2018. Chemical methods for mapping cysteine oxidation. Chem. Soc. Rev. 47 (1), 231–268.

Amiri, N.S., Hosseini, M.-R.-M., 2020. Application of ratiometric fluorescence sensor-based microwave-assisted synthesized CdTe quantum dots and mesoporous structured epitope-imprinted polymers for highly efficient determination of tyrosine phosphopeptide. Anal. Methods 12 (1), 63–72.

Amjadi, M., Jalili, R., 2017. Molecularly imprinted mesoporous silica embedded with carbon dots and semiconductor quantum dots as a ratiometric fluorescent sensor for diniconazole. Biosens. Bioelectron. 96, 121–126.

Annak, H. et al, 2007. Phosphate recognition in structural biology. Angew. Chem. Int. Ed. 46 (3), 338–352.

Bimberg, D., Grundmann, M., Ledentsov, N.N., 1999. Quantum dot heterostructures. John Wiley & Sons, Chichester.

Cai, X. et al, 2014. Chemodosimeter-based fluorescent detection of L-cysteine after extracted by molecularly imprinted polymers. Talanta 120, 297–303.

Chao, M.-R., Hu, C.-W., Chen, J.-L., 2014. Fluorescent turn-on detection of cysteine using a molecularly imprinted polyacrylate linked to allylthiol-capped CdTe quantum dots. Microchim. Acta 181 (9–10), 1085–1091.

Chen, W. et al, 2019. Protein recognition by polydopamine-based molecularly imprinted hollow spheres. Biosens. Bioelectron. 142, 111492.

Chen, S. et al, 2020. A phosphorescent probe for cephalexin consisting of mesoporous thioglycolic acid-modified Mn: ZnS quantum dots coated with a molecularly imprinted polymer. Microchim. Acta 187 (1), 1–10.

Dai, H. et al, 2020. Highly sensitive determination of 4-nitrophenol with coumarin-based fluorescent molecularly imprinted poly (ionic liquid). J. Hazard. Mater. 398, 122854.

Delaunay, N., Combès, A., Pichon, V., 2020. Immunoaffinity extraction and alternative approaches for the analysis of toxins in environmental, food or biological matrices. Toxins 12 (12), 795.

Demir, B. et al, 2018. Tracking hyaluronan: molecularly imprinted polymer coated carbon dots for cancer cell targeting and imaging. ACS Appl. Mater. Interfaces 10 (4), 3305–3313.

Dezfulian, C. et al, 2007. Role of the anion nitrite in ischemia-reperfusion cytoprotection and therapeutics. Cardiovasc. Res. 75 (2), 327–338.

Dickey, F.H., 1949. The preparation of specific adsorbents. PNAS 35 (5), 227.

Dickey, F.H., 1955. Specific adsorption. The Journal of Physical Chemistry 59 (8), 695–707.

Duke, R.M. et al, 2010. Colorimetric and fluorescent anion sensors: an overview of recent developments in the use of 1,8-naphthalimide-based chemosensors. Cheminform 39 (10), 3936–3953.

El-Schich, Z. et al, 2016. Different expression levels of glycans on leukemic cells—a novel screening method with molecularly imprinted polymers (MIP) targeting sialic acid. Tumor Biology 37 (10), 13763–13768.

El-Schich, Z. et al, 2021. Sialic acid as a biomarker studied in breast cancer cell lines in vitro using fluorescent molecularly imprinted polymers. Applied Sciences 11 (7), 3256.

Ensafi, A.A., Nasr-Esfahani, P., Rezaei, B., 2017. Simultaneous detection of folic acid and methotrexate by an optical sensor based on molecularly imprinted polymers on dual-color CdTe quantum dots. Anal. Chim. Acta 996, 64–73.

Feng, H. et al, 2014. Surface molecular imprinting on dye–(NH2)–SiO2 NPs for specific recognition and direct fluorescent quantification of perfluorooctane sulfonate. Sens. Actuators, B 195, 266–273.

Forsyth, A.B.D., 2002. Okadaic acid: the archetypal serine/threonine protein phosphatase inhibitor. Curr. Med. Chem. 9 (22).

Friedman, M., 2001. Application of the S-pyridylethylation reaction to the elucidation of the structures and functions of proteins. J. Protein Chem. 20 (6), 431–453.

Geddes, C.D., 2001. Optical halide sensing using fluorescence quenching: theory, simulations and applications - a review. Meas. Sci. Technol. 12 (9), R53.

Guo, Z. et al, 2014. Recent progress in the development of near-infrared fluorescent probes for bioimaging applications. Chem. Soc. Rev. 43 (1), 16–29.

Hammoud, H. et al, 2012. Direct guanidinylation of aryl and heteroaryl halides via copper-catalyzed cross-coupling reaction. J. Org. Chem. 77 (1), 417–423.

Han, J. et al, 2019. Systematic overview of aristolochic acids: nephrotoxicity, carcinogenicity, and underlying mechanisms. Front. Pharmacol. 10.

Hao, T. et al, 2016. An eco-friendly molecularly imprinted fluorescence composite material based on carbon dots for fluorescent detection of 4-nitrophenol. Microchim. Acta 183 (7), 2197–2203.

Haupt, K., Medina Rangel, P.X., Bui, B.T.S., 2020. Molecularly imprinted polymers: Antibody mimics for bioimaging and therapy. Chem. Rev. 120 (17), 9554–9582.

Henry, O.Y., Cullen, D.C., Piletsky, S.A., 2005. Optical interrogation of molecularly imprinted polymers and development of MIP sensors: a review. Anal. Bioanal. Chem. 382 (4), 947–956.

Hou, Y. et al, 2020. Biological sample-compatible ratiometric fluorescent molecularly imprinted polymer microspheres by RAFT coupling chemistry. Langmuir 36 (41), 12403–12413.

Huynh, T.-P. et al, 2013. Molecularly imprinted polymer for recognition of 5-fluorouracil by RNA-type nucleobase pairing. Anal. Chem. 85 (17), 8304–8312.

Jia, M. et al, 2017. A molecular imprinting fluorescence sensor based on quantum dots and a mesoporous structure for selective and sensitive detection of 2, 4-dichlorophenoxyacetic acid. Sens. Actuators, B 252, 934–943.

Jiang, X. et al, 2007. Small organic molecular imprinted materials: their preparation and application. Anal. Bioanal. Chem. 389 (2), 355–368.

Jiao, Z. et al, 2018. A molecularly imprinted chitosan doped with carbon quantum dots for fluorometric determination of perfluorooctane sulfonate. Microchim. Acta 185 (10), 1–9.

Jin, X. et al, 2018. A molecularly imprinted electrochemiluminescence sensor based on upconversion nanoparticles enhanced by electrodeposited rGO for selective and ultrasensitive detection of clenbuterol. Biosens. Bioelectron. 102, 357–364.

Johansson, E. et al, 2020. Pentavalent sialic acid conjugates block coxsackievirus A24 variant and human adenovirus type 37–viruses that cause highly contagious eye infections. ACS Chem. Biol. 15 (10), 2683–2691.

Ke, C.-B., Lu, T.-L., Chen, J.-L., 2020. Fluorometric determination of amifostine and alkaline phosphatase on amphiprotic molecularly imprinted silica crosslinked with binary functional silanes and carbon dots. Biosens. Bioelectron. 151, 111965.

Kimani, M. et al, 2021. Imprinted particles for direct fluorescence detection of sialic acid in polar media and on cancer cells with enhanced control of nonspecific binding. ACS Applied Polymer Materials 3 (5), 2363–2373.

Kingshott, P., Griesser, H.J., 1999. Surfaces that resist bioadhesion. Curr. Opin. Solid State Mater. Sci. 4 (4), 403–412.

Kunath, S. et al, 2015. Cell and tissue imaging with molecularly imprinted polymers as plastic antibody mimics. Adv. Healthcare Mater. 4 (9), 1322–1326.
Kupai, J. et al, 2017. Long-term stability and reusability of molecularly imprinted polymers. Polym. Chem. 8 (4), 666–673.
Lau, C., 2012. Perfluorinated compounds. EXS 101 (101), 47.
Leung, M.-K.-P., Chow, C.-F., Lam, M.-H.-W., 2001. A sol–gel derived molecular imprinted luminescent PET sensing material for 2, 4-dichlorophenoxyacetic acid. J. Mater. Chem. 11 (12), 2985–2991.
Li, D.-Y. et al, 2015. A "turn-on" fluorescent receptor for detecting tyrosine phosphopeptide using the surface imprinting procedure and the epitope approach. Biosens. Bioelectron. 66, 224–230.
Li, Z. et al, 2019. Fluorometric determination of ciprofloxacin using molecularly imprinted polymer and polystyrene microparticles doped with europium (III)(DBM) 3 phen. Microchim. Acta 186 (6), 334.
Li, Q. et al, 2020. Selective detection of phospholipids using molecularly imprinted fluorescent sensory core-shell particles. Sci. Rep. 10 (1), 1–7.
Li, M., Liu, H., Ren, X., 2017. Ratiometric fluorescence and mesoporous structured imprinting nanoparticles for rapid and sensitive detection 2, 4, 6-trinitrophenol. Biosens. Bioelectron. 89, 899–905.
Li, X., Plésiat, P., Nikaido, H., 2015. The challenge of efflux-mediated antibiotic resistance in gram-negative bacteria. Clin. Microbiol. Rev. 28 (2), 337–418.
Li, et al, 2010. Anion complexation and sensing using modified urea and thiourea-based receptors. Cheminform 39 (10), 3729–3745.
Li, j., et al, 2020. Detection of perfluorooctane sulfonate by molecularly imprinted upconversion fluorescent probe with mesoporous structure. Chin. J. Anal. Chem. 48 (11), 1493–1501.
Liang, L., Liu, Z., 2011. A self-assembled molecular team of boronic acids at the gold surface for specific capture of cis-diol biomolecules at neutral pH. Chem. Commun. 47 (8), 2255–2257.
Limaee, N.Y. et al, 2019. Selective 2, 4-dichlorophenoxyacetic acid optosensor employing a polyethersulfone nanofiber-coated fluorescent molecularly imprinted polymer. Polymer 177, 73–83.
Limaee, N.Y. et al, 2020. Selective recognition of herbicides in water using a fluorescent molecularly imprinted polymer sensor. Journal of Fluorescence 30 (2), 375–387.
Lin, J., Yamada, M., 2000. Chemiluminescent reaction of fluorescent organic compounds with KHSO5 using cobalt (II) as catalyst and its first application to molecular imprinting. Anal. Chem. 72 (6), 1148–1155.
Liu, R. et al, 2011. Core-shell nanostructured molecular imprinting fluorescent chemosensor for selective detection of atrazine herbicide. Analyst 136 (1), 184–190.
Liu, R. et al, 2017. Preparation of sialic acid-imprinted fluorescent conjugated nanoparticles and their application for targeted cancer cell imaging. ACS Appl. Mater. Interfaces 9 (3), 3006–3015.
Liu, G. et al, 2019. Recent advances and perspectives of molecularly imprinted polymer-based fluorescent sensors in food and environment analysis. Nanomaterials 9 (7), 1030.
Long, R. et al, 2019. Molecularly imprinted polymers coated CdTe quantum dots with controllable particle size for fluorescent determination of p-coumaric acid. Talanta 196, 579–584.
Lou, X. et al, 2012. An indirect approach for anion detection: the displacement strategy and its application. Chem. Commun. 48.
Lu, X. et al, 2020. Highly sensitive determination of 2, 4, 6-trichlorophenol by using a novel SiO2@ MIPIL fluorescence sensor with a double recognition functional monomer. ACS Sensors 5 (5), 1445–1454.
Mary, W. et al, 2018. Drinking water nitrate and human health: an updated review. Int. J. Environ. Res. Public Health 15 (7), 1557.
Meng, M. et al, 2019. Selective recognition of salicylic acid employing new fluorescent imprinted membrane functionalized with poly (amidoamine)(PAMAM)-encapsulated Eu (TTA) 3phen. J. Lumin. 208, 24–32.
Michl, J. et al, 2014. Naturally occurring aristolochic acid analogues and their toxicities. Nat. Prod. Rep. 31 (5), 676–693.
Panagiotopoulou, M. et al, 2016. Molecularly imprinted polymer coated quantum dots for multiplexed cell targeting and imaging. Angew. Chem. Int. Ed. 128 (29), 8384–8388.
Panagiotopoulou, M. et al, 2017. Fluorescent molecularly imprinted polymers as plastic antibodies for selective labeling and imaging of hyaluronan and sialic acid on fixed and living cells. Biosens. Bioelectron. 88, 85–93.
Pauling, L., Campbell, D.H., 1942. The manufacture of antibodies in vitro. J. Exp. Med. 76 (2), 211–220.
Piletska, E.V. et al, 2020. Combinatorial screening of polymer nanoparticles for their ability to recognize epitopes of AAV-neutralizing antibodies. J. Mol. Recognit. 33 (4), e2824.
Polyakov, M., 1931. Adsorption properties and structure of silica gel. Zhur Fiz Khim 2, 799–805.
Rajpal, S., Bhakta, S., Mishra, P., 2021. Biomarker imprinted magnetic core–shell nanoparticles for rapid, culture free detection of pathogenic bacteria. J. Mater. Chem. B 9 (10), 2436–2446.
Raksawong, P. et al, 2017. A hybrid molecularly imprinted polymer coated quantum dot nanocomposite optosensor for highly sensitive and selective determination of salbutamol in animal feeds and meat samples. Anal. Bioanal. Chem. 409 (20), 4697–4707.
Rangel, P.X.M. et al, 2019. Solid-phase synthesis of molecularly imprinted polymer nanolabels: affinity tools for cellular bioimaging of glycans. Sci. Rep. 9 (1), 1–9.
Ren, X.-H. et al, 2021. Preparation of glycan-oriented imprinted polymer coating Gd-doped silicon nanoparticles for targeting cancer Tn antigens and dual-modal cell imaging via boronate-affinity surface imprinting. Talanta 223, 121706.
Shi, T. et al, 2019. CdTe quantum dots coated with a molecularly imprinted polymer for fluorometric determination of norfloxacin in seawater. Microchim. Acta 186 (6), 1–8.
Shinde, S. et al, 2015. Sialic acid-imprinted fluorescent core-shell particles for selective labeling of cell surface glycans. J. Am. Chem. Soc. 137 (43), 13908–13912.
Silsirivanit, A., 2019. Glycosylation markers in cancer. Adv. Clin. Chem.
Singh, M. et al, 2020. *Recent advancement of carbon nanomaterials engrained molecular imprinted polymer for environmental matrix*. Trends in Environmental. Anal. Chem., e00092
Takeuchi, T., Goto, D., Shinmori, H., 2007. Protein profiling by protein imprinted polymer array. Analyst 132 (2), 101–103.
Tian, L. et al, 2021. Fabrication of a near-infrared excitation surface molecular imprinting ratiometric fluorescent probe for sensitive and rapid detecting perfluorooctane sulfonate in complex matrix. J. Hazard. Mater. 413, 125353.
Tirado-Guizar, A., Paraguay-Delgado, F., Pina-Luis, G.E., 2016. A molecularly imprinted polymer-coated CdTe quantum dot nanocomposite for tryptophan recognition based on the Förster resonance energy transfer process. Method. Appl. Fluoresc. 4, (4) 045003.
Ton, X.-A. et al, 2015. A disposable evanescent wave fiber optic sensor coated with a molecularly imprinted polymer as a selective fluorescence probe. Biosens. Bioelectron. 64, 359–366.
Turkewitsch, P. et al, 1998. Fluorescent functional recognition sites through molecular imprinting. A polymer-based fluorescent chemosensor for aqueous cAMP. Anal. Chem. 70 (10), 2025–2030.
Tva, B. et al, 2020. Application of molecularly imprinted polymers as artificial receptors for imaging. Acta Biomater. 101, 444–458.
Uzun, L. et al, 2013. Chiral recognition of proteins having L-histidine residues on the surface with lanthanide ion complex incorporated-molecularly imprinted fluorescent nanoparticles. Mater. Sci. Eng., C 33 (6), 3432–3439.
Wagner, R. et al, 2013. Synthesis, spectroscopic, and analyte-responsive behavior of a polymerizable naphthalimide-based carboxylate probe and molecularly imprinted polymers prepared thereof. The Journal of Organic Chemistry 78 (4), 1377–1389.

Wagner, S. et al, 2018. Integrating fluorescent molecularly imprinted polymer (MIP) sensor particles with a modular microfluidic platform for nanomolar small-molecule detection directly in aqueous samples. Biosens. Bioelectron. 99, 244–250.
Wan, W. et al, 2013. Fluorescent sensory microparticles that "light-up" consisting of a silica core and a molecularly imprinted polymer (MIP) shell. Angew. Chem. Int. Ed. 52 (27), 7023–7027.
Wan, W. et al, 2017. *Ratiometric fluorescence detection of phosphorylated amino acids through excited-state proton transfer by using molecularly imprinted polymer (MIP) recognition nanolayers*. Chemistry–A. European Journal 23 (63), 15974–15983.
Wang, X. et al, 2016. A molecular imprinting-based turn-on ratiometric fluorescence sensor for highly selective and sensitive detection of 2, 4-dichlorophenoxyacetic acid (2, 4-D). Biosens. Bioelectron. 81, 438–444.
Wang, S. et al, 2016. Targeting and imaging of cancer cells via monosaccharide-imprinted fluorescent nanoparticles. Sci. Rep. 6 (1), 1–11.
Wang, Z. et al, 2019. Molecularly imprinted polymers-coated CdTe quantum dots for highly sensitive and selective fluorescent determination of ferulic acid. Journal of Analytical Methods in Chemistry 2019.
Wang, J. et al, 2020. Co-precipitation method to prepare molecularly imprinted fluorescent polymer nanoparticles for paracetamol sensing. Colloids Surf., A 587, 124342.
Wang, M. et al, 2020. Composite material based on carbon dots and molecularly imprinted polymers: a facile probe for fluorescent detection of 4-nitrophenol. NANO 15 (08), 2050105.
Wang, F. et al, 2021. A simple approach to prepare fluorescent molecularly imprinted nanoparticles. RSC Adv. 11 (13), 7732–7737.
Wang, J., Qiu, J., 2016. A review of carbon dots in biological applications. J. Mater. Sci. 51 (10), 4728–4738.
Wang, Y., Wang, Y., Liu, H., 2019. A novel fluorescence and SPE adsorption nanomaterials of molecularly imprinted polymers based on quantum dot-grafted covalent organic frameworks for the high selectivity and sensitivity detection of ferulic acid. Nanomaterials 9 (2), 305.
Watanabe, N., Osada, H., 2016. Small molecules that target phosphorylation dependent protein-protein interaction. Bioorg. Med. Chem., 3246–3254
Wei, X. et al, 2015. Specific recognition and fluorescent determination of aspirin by using core-shell CdTe quantum dot-imprinted polymers. Microchim. Acta 182 (7–8), 1527–1534.
Wen, S. et al, 2018. Advances in highly doped upconversion nanoparticles. Nat. Commun. 9 (1), 1–12.
Whitcombe, M.J. et al, 2011. The rational development of molecularly imprinted polymer-based sensors for protein detection. Chem. Soc. Rev. 40 (3), 1547–1571.
Xu, X. et al, 2004. Electrophoretic analysis and purification of fluorescent single-walled carbon nanotube fragments. J. Am. Chem. Soc. 126 (40), 12736–12737.
Xu, S. et al, 2013. Dummy molecularly imprinted polymers-capped CdTe quantum dots for the fluorescent sensing of 2, 4, 6-trinitrotoluene. ACS Appl. Mater. Interfaces 5 (16), 8146–8154.
Xu, Z. et al, 2016. Fluorescent molecularly imprinted polymers based on 1, 8-naphthalimide derivatives for efficiently recognition of cholic acid. Mater. Sci. Eng., C 58, 558–567.
Xu, X. et al, 2018. Carbon dots coated with molecularly imprinted polymers: A facile bioprobe for fluorescent determination of caffeic acid. J. Colloid Interface Sci. 529, 568–574.
Xu, X. et al, 2020. Three-dimensional flower-like multifunctional adsorbents with excellent sorptive removal and colorimetric detection of arsenate. Chem. Eng. J. 398, 125649.
Xu, S., Zou, Y., Zhang, H., 2020. Well-defined hydrophilic "turn-on"-type ratiometric fluorescent molecularly imprinted polymer microspheres for direct and highly selective herbicide optosensing in the undiluted pure milks. Talanta 211, 120711.
Yan, H., Cheng, X., Sun, N., 2013. Synthesis of multi-core–shell magnetic molecularly imprinted microspheres for rapid recognition of dicofol in tea. J. Agric. Food. Chem. 61 (11), 2896–2901.
Yang, M. et al, 2013. Determination of ATP using a double-receptor sandwich method based on molecularly imprinted membrane and fluorescence-labeled uranyl–salophen complex. Anal. Bioanal. Chem. 405 (23), 7545–7551.
Yang, Y. et al, 2016. One-pot synthesis of quantum dot-labeled hydrophilic molecularly imprinted polymer nanoparticles for direct optosensing of folic acid in real, undiluted biological samples. Biosens. Bioelectron. 86, 580–587.
Yang, Q. et al, 2020. Rational construction of a triple emission molecular imprinting sensor for accurate naked-eye detection of folic acid. Nanoscale 12 (11), 6529–6536.
Yang, M. et al, 2021. A novel ascorbic acid ratiometric fluorescent sensor based on ZnCdS quantum dots embedded molecularly imprinted polymer and silica-coated CdTeS quantum dots. J. Mol. Liq. 337, 116438.
Ye, J. et al, 2020. Molecularly imprinted ratiometric fluorescent probe for visual and fluorescent determination of aristolochic acid I based on a Schiff-base fluorescent compound. Microchim. Acta 187 (11), 1–10.
Yuphintharakun, N. et al, 2018. A nanocomposite optosensor containing carboxylic functionalized multiwall carbon nanotubes and quantum dots incorporated into a molecularly imprinted polymer for highly selective and sensitive detection of ciprofloxacin. Spectrochim. Acta Part A Mol. Biomol. Spectrosc. 201, 382–391.
Zhang, W. et al, 2017. Transferrin-navigation nano artificial antibody fluorescence recognition of circulating tumor cells. Sci. Rep. 7 (1), 1–10.
Zhang, Z. et al, 2020. A fluorescence microplate assay based on molecularly imprinted silica coated quantum dot optosensing materials for the separation and detection of okadaic acid in shellfish. Chemosphere 246, 125622.
Zhu, R. et al, 2021. A functional ratio fluorescence sensor platform based on the graphene/Mn-ZnS quantum dots loaded with molecularly imprinted polymer for selective and visual detection sinapic acid. Spectrochim. Acta Part A Mol. Biomol. Spectrosc. 244, 118845.
Zoughi, S. et al, 2021. Detection of tartrazine in fake saffron containing products by a sensitive optical nanosensor. Food Chem. 350, 129197.
Zu, F. et al, 2017. The quenching of the fluorescence of carbon dots: a review on mechanisms and applications. Microchim. Acta 184 (7), 1899–1914.